

Experimental investigation of free decaying turbulence in a non-neutral plasma

G. Bettega¹, F. Cavaliere¹, M. Cavenago², F. De Luca¹, R. Pozzoli¹, M. Romé¹

¹ *I.N.F.N. Sez. di Milano and Dip. di Fisica, Università degli Studi di Milano, Milano, Italy*

² *I.N.F.N. Laboratori Nazionali di Legnaro, Legnaro, Italy*

Introduction

In a wide range of experimental parameters the transverse dynamics of an electron plasma confined in a Malmberg-Penning trap [1] turns out to be similar to that of a two-dimensional (2D) inviscid incompressible fluid. Here, results of the spectral analysis of the free decaying 2D turbulence in a pure electron plasma are presented and discussed in the context of well known theoretical models.

The experimental results have been obtained in the ELTRAP device [2], where an electron plasma generated by a hot tungsten filament (the plasma radius is 1–2 cm), is contained within a stack of hollow conducting cylinders with inner radius $R_w = 4.5$ cm, for a maximum plasma length of 80 cm. The apparatus is evacuated at a pressure of 10^{-9} mbar. The axial confinement is provided by biasing two electrodes at a voltage of -100 V, and the radial confinement by a highly uniform axial magnetic field $B \leq 0.2$ T directed along the axis of the trap. Electron densities $n = 10^6$ – 10^7 cm⁻³ and temperatures $T = 1$ – 10 eV are obtained. On the base of these parameters, the axial and the transverse dynamics turn out to be well separated in time and temperature effects are negligible, so that the plasma evolution can be modeled with the cold fluid drift-Poisson system [3]

$$\partial n / \partial t + \mathbf{v} \cdot \nabla n = 0, \quad \mathbf{v} = -\nabla \phi \times \mathbf{e}_z / B, \quad \nabla^2 \phi = en / \epsilon_0 \quad (1)$$

for the electron density n , the velocity field \mathbf{v} and the electrostatic potential ϕ ; SI units are used, with $-e$ the electron charge and ϵ_0 the vacuum permittivity. These equations contain only the $\mathbf{E} \times \mathbf{B}$ -drift dynamics, being \mathbf{E} the self-consistent electric field. The system (1) is isomorphic to the Euler system for a 2D ideal fluid [4], with a correspondence between the vorticity ζ and the plasma density, $\zeta = (e/\epsilon_0 B)n$, and between the fluid stream function and the electrostatic potential, $\psi = \phi/B$.

Experiments and data analysis

The device operates with cycles of plasma injection, hold and ejection. The electrons are detected by dumping them onto a phosphor screen kept at a voltage of ≈ 10 kV and collecting the

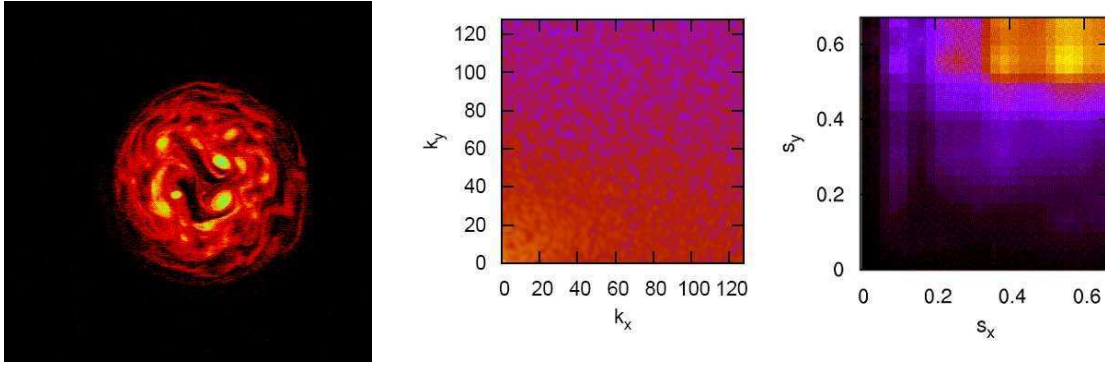


Figure 1: Left: snapshot of the plasma density distribution in a relaxed turbulent state. Center: 2D Fourier spectrum. Right: Morlet wavelet spectrum.

emitted light by a triggered high resolution CCD camera, obtaining a snapshot of the plasma axially averaged density distribution. The transverse plasma dynamics is reconstructed repeating machine cycles with an increasing trapping time, starting from the same initial condition. The initial evolution is dominated by the diocotron instability [4], due to the angular velocity shear in the initial density profile, which drives the plasma into a strongly non-linear regime, in which vortex structures appear. The free relaxation typically involves processes like advection, instabilities, filamentation and merger. The number of vortices decreases in time with a power law scaling [6]. A flow characterized by the presence of a coherent part made of long-living (hundreds of average plasma azimuthal rotation periods) high intensity vortices, often arranged in symmetric arrays (vortex crystals [5]), and of a turbulent background of low particle density, is experimentally observed (see Fig. 1-2, left).

In each point of the images the light intensity is proportional to the axially integrated plasma density. Solving the (normalized) Poisson equation $\nabla^2 \phi = n$ on a Cartesian grid, with the boundary condition $\phi(r = 1, t) = 0$ (r being normalized over R_w), the distribution of the electrostatic energy density $-(1/2)n\phi$ and other quantities of interest (like, e.g, the enstrophy density) can be obtained, and their time evolution analyzed.

In a standard Fourier analysis a generic discretized quantity, $V_{j,k}$, ($j, k = 0, \dots, N - 1$), is written in the form $V_{j,k} = \sum_{m=-m_{max}}^{m_{max}} \sum_{n=-n_{max}}^{n_{max}} V_{m,n} \exp(i2\pi m j/N) \exp(i2\pi n k/N)$, in which the summations are extended up to Nyquist limit $m_{max} = n_{max} = N/2$. In this way a 2D map is obtained representing the distribution of the spatial frequencies which are present in the energy distribution (see Fig. 1-2, center). Finally, starting from the map $V_{m,n}$ a one-dimensional (1D) spectrum is obtained summing the squares of the amplitudes corresponding to a constant modulus $k = \pi\sqrt{m^2 + n^2}$, $V(k) = [\sum_{|k|=\text{const}} |V_{m,n}|^2]^{1/2}$.

The presence of localized coherent structures introduces non negligible contributions at all

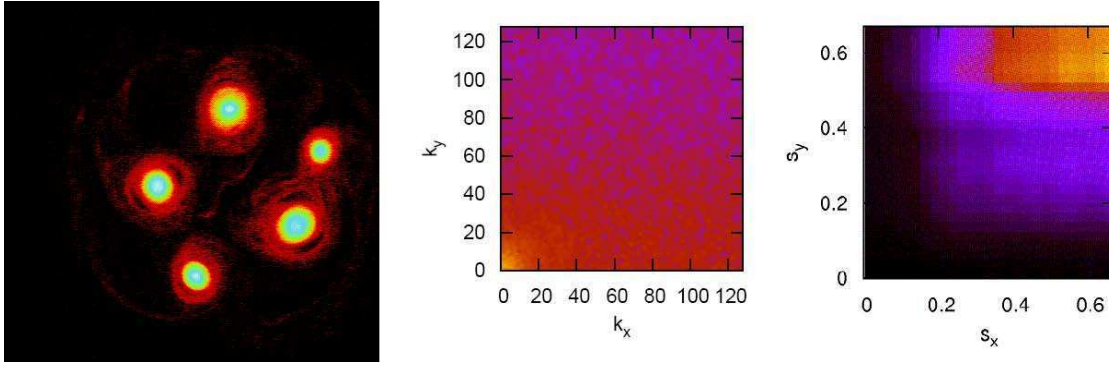


Figure 2: Left: snapshot of the plasma density distribution in a vortex crystal state. Center: 2D Fourier spectrum. Right: Morlet wavelet spectrum.

scales (wavenumbers) in the Fourier space, determining a piling-up effect at small spatial scales, so that the Fourier analysis is no longer a proper inspection tool. This difficulty can be removed using wavelet transforms. Wavelet coefficients are analogous to Fourier coefficients, and are calculated as the cross-correlation between the signal and a translated (by an amount a) and scaled (by a scale factor k , analogous to the Fourier wavenumber) version $\psi_{a,k}$ of a well localized in space (or time) base function ψ (the wavelet). A generic 2D quantity V is wavelet transformed along the x and y directions, obtaining the wavelet coefficients $V[x, s_x, y, s_y]$, being s_x and s_y the scales in the two spatial directions. A mean 2D map $(\langle |\tilde{V}(s_x, s_y)|^2 \rangle)^{1/2}$ is computed by integrating the square modulus of the coefficients over the space variables (see Fig. 1-2, right). The normalization of the wavelets is chosen in order to keep the same “energy” at all the discrete scales s_j , being $s_j = s_0 2^{j\delta}$. Here, s_0 is the minimum scale, δ sets the number of scales and $j = 0, \dots, J$, with $J = \delta^{-1} \log_2 N / s_0$. A 1D spectrum is obtained using the same technique used for the 2D Fourier map, summing the squares of the wavelet coefficients corresponding to a constant wavelet scale, and taking the square root of the result.

Discussion

The statistical theory of the 2D turbulence is due to Kraichnan [7] and Batchelor [8]. The theory of Kraichnan deals with the forced turbulence, in which energy is continuously injected in the fluid, while the theory of Batchelor deals with the free decaying turbulence, which is of interest in the present case. According to Batchelor, the 2D free relaxing turbulence is characterized by a power law enstrophy scaling, $E(k) \approx \beta^{2/3} k^{-3}$, where β is the enstrophy dissipation rate for unit volume. Fig. 3 shows the results for the 1D spectra of energy, for the data of Figs. 1-2. The spectra for a relaxed turbulent state and a state with vortex crystals show clear differences at small k (large spatial scales). The experimental data for the turbulent state qualitatively agree

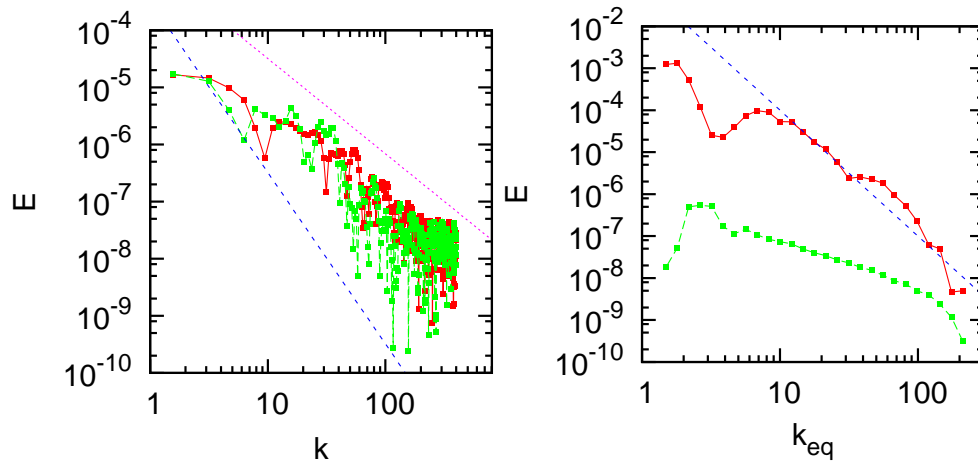


Figure 3: Energy spectra for the turbulent state (red line) and for the vortex crystal state (green line), computed with the Fourier analysis (left) and the wavelet analysis (right), for the data of Figs. 1-2; k_{eq} represents the equivalent Fourier wavenumber. On the left plot, the dotted lines represent the expected behavior of the energy spectrum for the free relaxing, k^{-3} , and the forced, $k^{-5/3}$, 2D turbulence. The dotted line on right plot is a line $\propto k^{-3}$. The scales of $E(k)$ are different because of the different normalizations used for the spectra.

with the enstrophy scaling for about one decade in both types of analysis. The Fourier spectrum tends to flatten at high spatial wavenumbers due to the difficulty of resolving small spatial scales.

References

- [1] J. H. Malmberg and J. S. deGrassie, Phys. Rev. Lett. **35**, 577 (1975).
- [2] M. Amoretti, G. Bettega, F. Cavaliere, M. Cavenago, F. De Luca, R. Pozzoli and M. Romé, Rev. Scient. Instrum. **74**, 3991 (2003).
- [3] C. F. Driscoll and K. S. Fine, Phys. Fluids B **2**, 1359 (1990).
- [4] R. H. Levy, Phys. Fluids **8**, 1288 (1965).
- [5] K. S. Fine, A. C. Cass, W. G. Flynn and C. F. Driscoll, Phys. Rev. Lett. **75**, 3277 (1995).
- [6] G. F. Carnevale, J. C. McWilliams, Y. Pomeau, J. B. Weiss and W. R. Young, Phys. Rev. Lett. **66**, 2735 (1991).
- [7] R. H. Kraichnan, Phys. Fluids **10**, 1417 (1967).
- [8] G. K. Batchelor, Phys. Fluids **12**, 233 (1969).